COLOR-BASED SKIN SEGMENTATION: AN EVALUATION OF THE STATE OF THE ART

Frerk Saxen, Ayoub Al-Hamadi

Otto von Guericke University Magdeburg
Institute for Information Technology and Communications
{Frerk.Saxen, Ayoub.Al-Hamadi}@ovgu.de

ABSTRACT

Skin segmentation is widely used, e.g. in face detection and gesture recognition. In the last years, the number of skin segmentation approaches has grown. However, multiple datasets and varying performance measurements make direct comparison difficult. We address these shortcomings and evaluate 5 threshold-based methods, 5 model-based methods, and 2 region-based state-of-the-art skin segmentation methods. We discuss each algorithm and provide the segmentation performance along with the processing time. All methods are evaluated on the ECU dataset which provides a great amount of training data besides other important attributes.

1. INTRODUCTION

Detecting human skin is rarely the final aim, but it is part of many applications. Among others, in face detection, gesture recognition, finding naked people, and hand sign recognition. The difficulties of skin segmentation have been mentioned early [1] (arbitrary background, unknown lighting conditions and camera calibration, highly variable shape and appearance of skin regions, and different skin tones).

Versatile datasets have been created to cover these attributes and plenty algorithms have been proposed to solve the task. However, basic questions such as "How well do current skin segmentation algorithms work?", "What is the best approach?", "Which datasets are available?", "Which should be preferred?" are not answered easily.

In our study we address these questions. We evaluate 5 threshold-based methods, 5 model-based methods, and 2 region-based methods. Threshold-based methods provide simple decision rules and are easy to implement. This attributes led to a vast use of threshold-based methods in the literature, although most have been evaluated poorly. Model-based methods need training and testing procedures and thus require datasets. Threshold-based methods and model-based methods use single pixel information only. Region-based methods incorporate neighbouring pixels and are often computational expensive and hence only scarcely used.

Our study extends the work of Vezhnevets *et al.* [2], Xu and Zhu [3], Schmugge *et al.* [4], Kelly *et al.* [5], and Kakumanu *et al.* [6]. We evaluate the best performing and most often used methods for skin segmentation.

2. SKIN SEGMENTATION METHODS

This section describes skin segmentation methods that are used in the following evaluation. We implemented each algorithm based on the original publication considering the parameter settings provided by the authors. Threshold-based methods provide decision rules for skin segmentation, generally based on thresholds. Model-based methods provide a formula for training and testing the skin segmentation approach. All model-based algorithms provide a threshold τ, which is determined in the 10-fold cross validation.

2.1. Model-based Methods

The **Bayes** approach for skin segmentation has been introduced by Jones and Rehg [8]. It assumes that a dataset provides enough samples to model the probability $P(\text{skin} \mid c)$ that a given color c belongs to skin by using the relative frequency of skin color observations. The Bayes'theorem is used to model the probability

$$P(\text{skin} \mid c) = \frac{P(c \mid \text{skin})P(\text{skin})}{P(c)} = \frac{\frac{n(c,X_{\text{skin}})}{N(X_{\text{skin}})} \frac{N(X_{\text{skin}})}{N(X)}}{\frac{n(c,X)}{N(X)}}, \quad (1)$$

where X denotes all (skin and non-skin) samples of the training set and X_{skin} all skin samples of the training set. $n(c, X)$ denotes how often the color c is observed in X and $N(X)$ are the total number of samples in X. The color c is considered as skin pixel if

$$\frac{n(c, X_{\text{skin}})}{n(c, X)} \geq \tau_{\text{Bayes}}. \quad (2)$$

The relative frequency can be stored in a lookup table (LUT) for every possible color value c for fast segmentation. Using the RGB color space, 256^3 possibilities must be stored in

---

the LUT. Phung *et al.* [7] have used color quantization to reduce the LUT space. Using only 32^3 bins requires 512 times less memory without noticeable loss in segmentation performance. The effect of color-transformation has been investigated by Shin *et al.* [9] and Kakumanu *et al.* [6], who recommended to use the original color space of the dataset because "histogram-based methods are not affected by the color space representation" [6]. Even though Shin *et al.* have shown that dropping the illuminant component results in a loss in segmentation performance, using 2D color spaces (e.g. the normalized RGB color space) is still prevalent in the literature.

Gaussian models provide the skin distribution using the probability density function (pdf). The mean μ and the co-variance matrix Σ are computed from all skin samples X_{skin} of the training set. A given pixel color c belongs to skin if the pdf exceeds the threshold τ_{Gauss}

$$(2\pi)^{-\frac{3}{2}} \, |\Sigma|^{-\frac{1}{2}} \, e^{-\frac{1}{2}(c-\mu)^T \Sigma^{-1}(c-\mu)} \geq \tau_{\text{Gauss}}. \qquad (3)$$

Phung *et al.* [7] have shown that using 3D Gaussian improves the segmentation performance. We evaluate a uni-modal skin pdf because it is dominant in the literature. For an elaborate evaluation of Gaussian models (including mixture of Gaussians) we refer to Phung *et al.* [7].

DSSD (Dempster-Shafer based Skin Detection) has been proposed and improved by Shoyaib *et al.* [10, 11]. It handles the uncertainties of threshold-based methods using the Dempster-Shafer (DS) theory of evidence. Six threshold-based methods (which are called source of informations (SoIs)) are weighted by skin and non-skin mass values m^{skin}, and $m^{\text{non-skin}}$. Table 1 shows the SoIs with skin and non-skin weights. We use simplifications from Barnett [12] to reduce the computational complexity from $O(3^n)$ to $O(n)$ without applying approximations, where $n = 6$ denotes the number of SoIs. The uncertainties

$$\Theta^{\text{skin}} = \prod_{i=1}^{n} \begin{cases} 1 - m_i^{\text{skin}}, & \text{if } SOI_i \text{ is true} \\ 1, & \text{otherwise} \end{cases}, \qquad (4)$$

$$\Theta^{\text{non-skin}} = \prod_{i=1}^{n} \begin{cases} 1 - m_i^{\text{non-skin}}, & \text{if } SOI_i \text{ is false} \\ 1, & \text{otherwise} \end{cases} \qquad (5)$$

could be compared directly (as proposed from Shoyaib *et al.* [11]). We divide $\Theta^{\text{non-skin}}$ by Θ^{skin} and map the result to use a threshold τ_{DSSD}, which ranges between 0 and 1. Thus, a given pixel belongs to skin if

$$\frac{2}{1 + e^{-\frac{\Theta^{\text{non-skin}}}{\Theta^{\text{skin}}}}} - 1 \geq \tau_{\text{DSSD}}. \qquad (6)$$

The equation can be rewritten so that only a single comparison $\hat{\tau}_{\text{DSSD}} \cdot \Theta^{\text{skin}} \geq \Theta^{\text{non-skin}}$ must be performed. Besides the usage of uncertainties, an advantage of *DSSD* is that an expensive training procedure is not necessary because the mass

values are provided from Shoyaib *et al.* [11]. Due to its generalization *DSSD* has shown improved segmentation performance for small training data [11]. Additionally, we trained mass values, which refer to *DSSDTrained* in our evaluation.

SoI	m^{skin}	$m^{\text{non-skin}}$
$R > 140$	0.364339536	0.524533342
$75 < G < 193$	0.147315460	0.430099211
$43 < B < 161$	0.222264545	0.440255872
$25 < |R - G| < 130$	0.546243640	0.675261991
$45 < |R - B| < 187$	0.496808781	0.673853774
$R > G \wedge R > B$	0.387888000	0.968090001

Table 1. Source of interests (SoI) with corresponding skin and non-skin mass values from Shoyaib *et al.* [11]

GDSSD is the generalized DSSD method (provided by Shoyaib *et al.* [11]). The equations for multiplying uncertainties and segmentation (Eq. 4, 5, 6) remain unchanged, but the threshold τ_{GDSSD} is used. The source of interests (SoIs) are not thresholded anymore. For example, SOI_4 becomes $|R - G|$. Instead, for every particular $|R - G|$ value a SoI is employed. This SoI_4 belongs to skin, i.e. SoI_4 is true, if

$$n(|R - G|, X_{\text{skin}}) > n(|R - G|, X_{\text{non-skin}}), \qquad (7)$$

where $n(c, X_{\text{skin}})$ denotes how often c is observed in the skin training set X_{skin}. $X_{\text{non-skin}}$ denotes the training set containing only non-skin samples. Thus, for every $|R - G|$ value a skin and a non-skin mass value is necessary. The *GDSSD* method is similar to the *Bayes* approach but requires less memory. Shoyaib *et al.* [11] have shown that the *GDSSD* method can outperform *Bayes* for a small data set.

2.2. Threshold-based Methods

Threshold-based skin segmentation methods are very popular. About one-third of our reviewed applications use threshold-based methods. The advantages are two-fold. First, it is not necessary to train a threshold-based method. Hence, the efforts in finding datasets and implementing training procedures can be omitted. Second, threshold-based methods are computationally efficient and easy to implement. The lower performance of threshold-based methods and the lack of adjustable thresholds are the disadvantages. We emphasize the first author with the year of publication to provide a unique name in the evaluation.

The *Chai1999* method [13] considers only the chrominance components of the YC_rC_b color space. A given pixel belongs to skin if

$$133 < C_r < 173 \wedge 77 < C_b < 127. \qquad (8)$$

Soriano2000 [14] intersects two quadratic functions in the normalized RGB (nRGB) color space. A skin pixel is detected if

$$g_{\text{down}} < nG < g_{\text{up}} \wedge W_r > 0.004, \qquad (9)$$

where the lower quadratic equations $g_{\text{down}} = -0.7279 * nR^2 + 0.6066 * nR + 0.1766$ and the upper equation $g_{\text{up}} = -1.8423 * nR^2 + 1.5294 * nR + 0.0422$. The white pixel ($nR = 0.33, nG = 0.33$) is excluded in Eq. 9 with $W_r = (nR - 0.33)^2 + (nG - 0.33)^2$.

Hsieh2002 [15] provides three empirically obtained zones for human skin segmentation in the HSI color space. The pixel is classified as skin if

$$
\begin{aligned}
I > 40 \wedge [(1 < H < 28 \wedge 13 < S < 110) \vee \\
(-28 < H < 0 \wedge 13 < S < 110) \vee \\
(-51 < H < -29 \wedge 13 < S < 75)] . \quad (10)
\end{aligned}
$$

Kovač2003 *et al.* [16] proposes a method for uniform daylight illumination, wich classifies a skin pixel if

$$
\begin{aligned}
R > 95 \wedge G > 40 \wedge B > 20 \wedge \\
max(R, G, B) - min(R, G, B) > 15 \wedge \\
|R - G| > 15 \wedge R > G \wedge R > B . \quad (11)
\end{aligned}
$$

Cheddad2009 [17] calculates a unimodal Gaussian in a one-dimensional error signal e and provides the thresholds $\mu - \sigma$ and $\mu + 3\sigma$ respectively. A skin pixel is detected if

$$
6.4031 \leq e \leq 30.0135, \quad (12)
$$

where $e = 0.2989R + 0.5870G + 0.1402B - max(G, B)$.

2.3. Region-based Methods

Region-based methods often need seed points, which are commonly taken from pixel-based methods. In our experiments, we use *BayesRGB32*[3] to provide seed points since it provides the best segmentation performance (see Fig. 1).

GraphCut has been used for skin segmentation, e.g. by Pierrard and Vetter [19] and Khan *et al.* [20]. The *GraphCut* algorithm minimizes the energy function

$$
E(L) = \sum_{p \in \mathcal{P}} D_p(L_p) + \sum_{(p,q) \in \mathcal{N}} K(p, q) \cdot T(L_p \neq L_q), \quad (13)
$$

where $L = \{L_p \mid p \in P\}$ is a labelling of image $\mathcal{P}$, p is a pixel of image $\mathcal{P}$, $L_p \in \{\mathcal{S}, \mathcal{T}\}$ is the label at pixel p, $\mathcal{S}$ is the skin label and $\mathcal{T}$ the non-skin label. $D_p(\cdot)$ is a data penalty function, $K(p, q)$ is a cost function of neighbourhood pixels p and q, $\mathcal{N}$ is the set of neighbour pixels (8-connected neighbourhood) and $T(\phi)$ is 1 if the statement ϕ is true or 0 otherwise. We set $K(p, q) = 1$ because calculating neighbourhood distances did not increase the segmentation performance. The probability $P(\text{skin} \mid c_p)$ that a color c_p of pixel p belongs to skin is provided by the *Bayes* approach (left-hand side of Eq. 2) and models the data penalty function

$$
D_p = \begin{cases} -\lambda \cdot log\left(P(\text{skin} \mid c_p)\right), & \text{if } L_p = \mathcal{S} \\ -\lambda \cdot log\left(2\tau_{\text{Bayes}} - P(\text{skin} \mid c_p)\right), & \text{if } L_p = \mathcal{T} \end{cases}, \quad (14)
$$

where λ, which has been chosen empirically, is set to 1.

Region Growing is a common image segmentation method and used for skin segmentation by Al-Wadud *et al.* [21]. An ambiguous pixel is segmented according to its unambiguous neighbourhood pixels. First, the *Bayes* approach provides a skin probability map $H(\mathcal{P})$ for image $\mathcal{P}$, by calculating the skin probability of every pixel $p \in \mathcal{P}$ using the left-hand side of Eq. 2. $H(\mathcal{P})$ can be thresholded with $\tau_U = 0.3\tau_{\text{Bayes}} + 0.7$ to obtain unambiguous skin pixels (seeds) $H(\mathcal{P}) > \tau_U$. Unambiguous non-skin seed pixels are obtained thresholding $H(\mathcal{P}) < \tau_L$, where $\tau_L = 0.15\tau_{\text{Bayes}}$. Ambiguous pixels satisfy $\tau_L \leq H(\mathcal{P}) \leq \tau_U$ and are determined in the later steps. Second, the gradient magnitude $M = \sqrt{D_x(\mathcal{P})^2 + D_y(\mathcal{P})^2}$ is calculated using the derivations $D_x(\mathcal{P})$ and $D_y(\mathcal{P})$ that are computed by convolving a 5×5 Sobel operator with the skin probability map $H(\mathcal{P})$. Third, all ambiguous neighbourhood pixels (8-connected neighbourhood) of the skin and non-skin seeds initialize the queue Q. Fourth, the queue Q is sorted according to its containing pixels gradient magnitude value M. Fifth, the pixel with the lowest gradient magnitude value M in queue Q belongs to skin if more of its neighbour pixels belong to skin than to non-skin. Otherwise it is classified as non-skin. Sixth, all ambiguous neighbourhood pixels of the classified pixel are added to queue Q. Steps four to six are repeated until queue Q is empty and all pixels have been classified. Al-Wadud *et al.* [21] searched for significant local minima of the histogram of $H(\mathcal{P})$ to determine τ_L and τ_U. We instead used τ_{Bayes} and varied the weights (i.e. 0.3 for τ_U and 0.15 for τ_L) to find the optimal thresholds but gained only slight improvements in the segmentation performance. Using the gradient magnitude of the image instead of the gradient magnitude of the probability map decreases the segmentation performance by 10% (using F-Measure and the ECU database [7] with 10-fold cross validation).

3. EVALUATION

Section 3.1 provides the chosen dataset along with statistics. The results of the evaluation are given in Section 3.2.

3.1. Datasets

Several datasets for skin segmentation are publicly available. In the following, we discuss the advantages and drawbacks of the most important and frequently used datasets. All datasets provide natural images with arbitrary background in indoor and outdoor scenes. Different lighting conditions are provided and various cameras have been used.

Jones and Regh [8] published in 1999 the Compaq dataset containing 13640 images ($80 \cdot 10^6$ skin, $855 \cdot 10^6$ non-skin pixels). It is still one of the largest datasets for skin segmentation and widely used in literature. The main drawback is the semi-automatic ground truth generation, which result in some
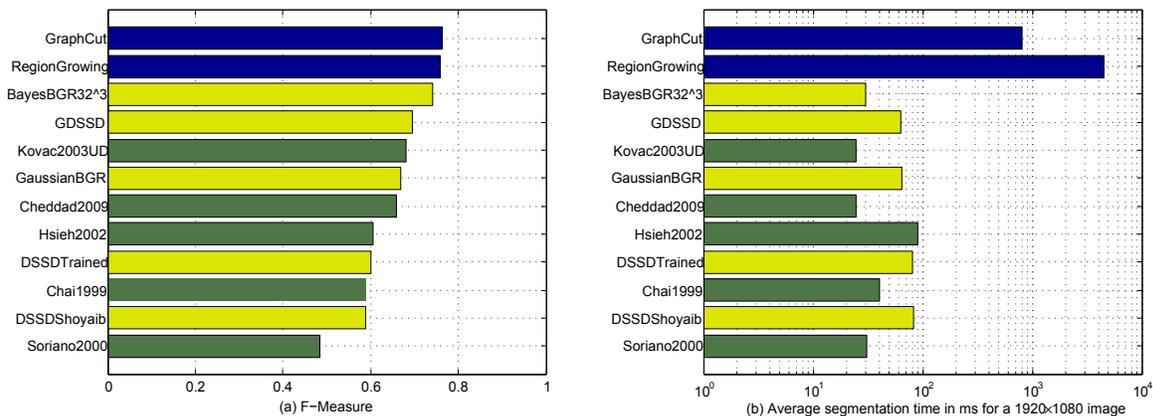
Fig. 1. Comparison of color-based skin segmentation methods (yellow: model-based, green: threshold-based, blue: region-based). (a) Segmentation performance of the described algorithms. (b) Average segmentation time for a 1920×1080 image.

bad annotations. Another disadvantage is the bad quality of many images.

Sigal *et al.* [22] proposed in 2004 the PAMI dataset with 21 videos cut from Hollywood films, where every 5th frame is annotated ($8.8 \cdot 10^6$ skin, $129 \cdot 10^6$ non-skin pixels). Ambiguous areas are annotated as "don't care" areas because a pixel based annotation is often hard to perform on border areas between skin and non-skin. The drawbacks are the small size of the dataset and the rare usage in the literature.

Phung *et al.* [7] provided in 2005 the ECU database with annotations of 4000 images ($209 \cdot 10^6$ skin, $902 \cdot 10^6$ non-skin pixels). Different skin types are covered as well as various indoor and outdoor lighting conditions. Accurate pixel annotations are provided. The ECU dataset is the largest database for skin segmentation and well organized but unfortunately not often used in the literature.

For our evaluation we chose the ECU dataset [7] because it is the largest skin segmentation dataset, provides accurate pixel annotations, and covers versatile attributes (e.g. background, lighting conditions, skin tones). The *Bayes*, *Gaussian*, and *Chai1999* method have already been evaluated by Phung *et al.* [7] and we obtained the same results.

We use F-Measure and 10-fold cross-validation to evaluate the skin segmentation methods.

3.2. Results

Fig. 1 shows the results. We implemented all methods in C++[1] and evaluated the algorithms on a PC (Intel Core i7 - 4×3.5 GHz). For *DSSDShoyaib* we used available parameters from the authors and for *DSSDTrained* we trained a new model. *GraphCut*, *Region Growing* and Bayes provide similar results and outperform other methods. *GraphCut* performs well for many images compared to *Bayes* but some-

times fails when big areas of the provided seed points from the *Bayes* approach hardly exceed the threshold τ_{Bayes}. Also *Region Growing* outperforms *Bayes* hardly because the skin probability map often provides small edges between skin and non-skin regions, resulting in a large growing procedure.

The *Bayes* method is one order of magnitude faster than its competitors and is one of the best performing methods. Since every possible color value is stored in a lookup table, it could be expected that *Bayes* performs best among all pixel-based methods. The number of labeled pixels in the dataset is crucial for the performance of the lookup table approach, since Shoyaib *et al.* [11] have shown that *DSSD* and *GDSSD* can outperform *Bayes* for smaller datasets.

4. CONCLUSION

Automatically detecting skin in images is used in many applications and often a time critical part of a larger task. This explains the popularity of threshold-based methods and the lack of evaluation studies. We addressed these shortcomings and provided an evaluation of state-of-the-art methods along with detailed descriptions of the algorithms. When possible, we used the parameters provided by the authors. We reviewed publicly available datasets for skin segmentation.

All methods reviewed in this paper are based solely on color information. The methods that are based on texture are applicable for a limited range of scales and will be addressed in future work. Further research might consider superpixels [24] for grouping pixels to reduce the sample size and to allow estimating the scale for texture analysis.

Using a dataset with only a single subject improves the segmentation performance for this individual. Detecting the face to individualize the skin classifier according to each subject can also improve the performance [25]. However, we focus on the basic methods for generic datasets in our evaluation.

---

[1]Please contact the authors to obtain the source code.

5. REFERENCES

[1] Rick Kjeldsen and John Kender, "Finding skin in color images," in *Second International Conference on Automatic Face and Gesture Recognition*. 1996, pp. 312–317, IEEE.

[2] Vladimir Vezhnevets, Vassili Sazonov, and Alla Andreeva, "A survey on pixel-based skin color detection techniques," in *GraphiCon*, 2003.

[3] Zhanwu Xu and Miaoliang Zhu, "Color-based skin detection: survey and evaluation," in *12th International Multi-Media Modelling*. 2006, pp. 143–152, IEEE.

[4] Stephen J. Schmugge, Sriram Jayaram, Min C. Shin, and LeonidV. Tsap, "Objective evaluation of approaches of skin detection using roc analysis," *Computer Vision and Image Understanding*, vol. 108, pp. 41–51, 2007.

[5] Wayne Kelly, Andrew Donnellan, and Derek Molloy, "A review of skin detection techniques for objectionable images," in *Information Technology and Telecommunication Conference (IT&T)*, Gabriel-Miro Muntean, Markus Hofmann, and Brian Nolan, Eds. 2007, pp. 40–49, IEEE.

[6] P. Kakumanu, S. Makrogiannis, and N. Bourbakis, "A survey of skin-color modeling and detection methods," *Pattern Recognition*, vol. 40, no. 3, pp. 1106–1122, 2007.

[7] Son Lam Phung, Abdesselam Bouzerdoum, and Douglas Chai, "Skin segmentation using color pixel classification: Analysis and comparison," *IEEE Transactions on Pattern Analysis and Machine Intelligence (PAMI)*, vol. 27, no. 1, pp. 148–154, 2005.

[8] Michael J. Jones and James M. Rehg, "Statistical color models with application to skin detection," in *Computer Vision and Pattern Recognition (CVPR)*. 1999, vol. 1, IEEE.

[9] Min C. Shin, Kyong I. Chang, and Leonid V. Tsap, "Does colorspace transformation make any difference on skin detection?," in *Applications of Computer Vision (WACV)*. 2002, pp. 275–279, IEEE.

[10] Mohammad Shoyaib, Mohammad Abdullah-Al-Wadud, and Oksam Chae, "A reliable skin detection using dempster-shafer theory of evidence," in *Computational Science and its Applications (ICCSA)*. 2009, vol. 5593 of *LNCS*, pp. 764–779, Springer-Verlag Berlin, Heidelberg.

[11] Mohammad Shoyaib, M. Abdullah-Al-Wadud, and Oksam Chae, "A skin detection approach based on the dempster-shafer theory of evidence," *International Journal of Approximate Reasoning*, vol. 53, no. 4, pp. 636–659, 2012.

[12] Jeffrey A. Barnett, "Computational methods for a mathematical theroy of evidence," in *Seventh International Conference on Artificial Intelligence*, 1981, pp. 868–875.

[13] Douglas Chai and King N. Ngan, "Face segmentation using skin colour map in videophone applications," *IEEE Transactions on Circuits and Systems for Video Technology*, vol. 9, no. 4, pp. 551–564, 1999.

[14] Maricor Soriano, Birgitta Martinkauppi, Sami Huovinen, and Mika Laaksonen, "Skin detection in video under changing illumination conditions," in *15th International Conference on Pattern Recognition (ICPR)*. 2000, vol. 1, pp. 839–842, IEEE.

[15] Ing-Sheen Hsieh, Kuo-Chin Fan, and Chiunhsiun Lin, "A statistic approach to the detection of humanfaces in colornaturescene," *Pattern Recognition*, vol. 35, no. 7, pp. 1583–1596, 2002.

[16] Jure Kovač, Peter Peer, and Frank Solina, "Human skin colour clustering for face detection," in *International Conference on Computer as a Tool EUROCON*, 2003.

[17] Abbas Cheddad, Joan Condell, Kevin Curran, and Paul Mc Kevitt, "A new color space for skin tone detection," in *Internation Conference on Image Processing (ICIP)*, 2009, pp. 497–500.

[18] Yuri Boykov and Vladimir Kolmogorov, "An experimental comparison of min-cut/max- flow algorithms for energy minimization in vision," *IEEE Transactions on Pattern Analysis and Machine Intelligence (PAMI)*, vol. 26, no. 9, pp. 1124–1137, 2004.

[19] Jean-Sébastien Pierrard and Thomas Vetter, "Skin detail analysis for face recognition," in *Conference on Computer Vision and Pattern Recognition (CVPR)*. 2007, pp. 1–8, IEEE.

[20] Rehan Ullah Khan, Allan Hanbury, and Julian Stöttinger, "Weighted skin color segmentation and detection using graph cuts," in *15th Computer Vision Winter Workshop (CVWW)*, 2010, pp. 107–114.

[21] M. Abdullah-Al-Wadud, Mohammad Shoyaib, and Oksam Chae, "A skin detection approach based on color distance map," *EURASIP Journal on Advances in Signal Processing*, vol. 2008, no. 814283, pp. 1–10, 2008.

[22] Leonid Sigal, Stan Sclaroff, and Vassilis Athitsos, "Skin color-based video segmentation under time-varying illumination," *IEEE Transactions on Pattern Analysis and Machine Intelligence*, vol. 26, no. 7, pp. 862–877, 2004.

[23] Christian Liensberger, Julian Stottinger, and Martin Kampel, "Color-based and context-aware skin detection for online video annotation," in *International Workshop on Multimedia Signal Processing (MMSP)*. 2009, IEEE.

[24] Peer Neubert and Peter Protzel, "Evaluating superpixels in video: Metrics beyond figure-ground segmentation," in *British Machine Vision Conference (BMVC)*, 2013.

[25] Heung-Il Suk, Bong-Kee Sin, and Seong-Whan Lee, "Hand gesture recognition based on dynamic bayesian network framework," *Pattern Recognition*, vol. 43, no. 9, pp. 3059–3072, 2010.